Influences of boreal fire emissions on Northern Hemisphere atmospheric carbon and carbon monoxide

Eric S. Kasischke,[1] Edward J. Hyer,[1] Paul C. Novelli,[2] Lori P. Bruhwiler,[2] Nancy H. F. French,[3] Anatoly I. Sukhinin,[4] Jennifer H. Hewson,[1] and Brian J. Stocks[5]

Received 24 May 2004; revised 19 November 2004; accepted 20 December 2004; published 16 February 2005.

[1] There were large interannual variations in burned area in the boreal region (ranging between 3.0 and 23.6 $\times$ 10^6 ha yr^{-1}) for the period of 1992 and 1995–2003 which resulted in corresponding variations in total carbon and carbon monoxide emissions. We estimated a range of carbon emissions based on different assumptions on the depth of burning because of uncertainties associated with the burning of surface-layer organic matter commonly found in boreal forest and peatlands, and average total carbon emissions were 106–209 Tg yr^{-1} and CO emissions were 33–77 Tg CO yr^{-1}. Burning of ground-layer organic matter contributed between 46 and 72% of all emissions in a given year. CO residuals calculated from surface mixing ratios in the high Northern Hemisphere (HNH) region were correlated to seasonal boreal fire emissions in 8 out of 10 years. On an interannual basis, variations in area burned explained 49% of the variations in HNH CO, while variations in boreal fire emissions explained 85%, supporting the hypotheses that variations in fuels and fire severity are important in estimating emissions. Average annual HNH CO increased by an average of 7.1 ppb yr^{-1} between 2000 and 2003 during a period when boreal fire emissions were 26 to 68 Tg CO^{-1} higher than during the early to mid-1990s, indicating that recent increases in boreal fires are influencing atmospheric CO in the Northern Hemisphere.

Citation: Kasischke, E. S., E. J. Hyer, P. C. Novelli, L. P. Bruhwiler, N. H. F. French, A. I. Sukhinin, J. H. Hewson, and B. J. Stocks (2005), Influences of boreal fire emissions on Northern Hemisphere atmospheric carbon and carbon monoxide, *Global Biogeochem. Cycles*, *19*, GB1012, doi:10.1029/2004GB002300.

1. Introduction

[2] Biomass burning has long been recognized as a significant source of a number of important trace gas species and particulate matter to the atmosphere [*Seiler and Crutzen*, 1980; *Lavoue et al.*, 2000; *Andreae and Merlet*, 2001]. Initially, fire emissions calculations were based on assessments of average burned area (using data reported by fire management agencies or best guesses) combined with average biomass levels (for different regions/biomes) and estimates of fraction of biomass consumed during fires. This procedure produced estimates of 2.55 Gt C yr^{-1} from global wildland fires and 3.86 Gt C yr^{-1} from all biomass-burning sources (including combustion of biofuels and charcoal and charcoal production) [*Andreae and Merlet*, 2001].

[3] Availability of satellite-based fire products has improved emission estimates from wildland fires. Three basic approaches are used: (1) hot spot detection [*Arino et al.*, 2001; *Giglio et al.*, 2000; *Justice et al.*, 2002; *Sukhinin et al.*, 2004], (2) burn scar mapping [*Tansey et al.*, 2004; *Simon et al.*, 2004], and (3) observation of atmospheric aerosols from fires [*Duncan et al.*, 2003a]. While hot spot products are the most widely available products and cover the longest time periods, caution must be exercised in using these data to estimate emissions [e.g., *Schultz*, 2002] because of sampling biases [*Eva and Lambin*, 1998; *Kasischke et al.*, 2003]. In some cases, hot spot data have been scaled to burned-area estimates by using other burned-area information [*Van der Werf et al.*, 2003].

[4] The new satellite data products are being used to estimate spatial and temporal patterns of burned area and are combined with data sets depicting spatial variations in biomass and fuel load to estimate emissions. Using a combination of satellite fire products, *Van der Werf et al.* [2004] estimated that an annual average of 3.53 Gt C yr^{-1} were released from wildland fires from 1997 to 2001, while *Ito and Penner* [2004] and *Hoelzemann et al.* [2004] estimated that 1.43 and 1.78 Gt C, respectively, were released from wildland fires in 2000.

[5] In this paper we present the results from a study aimed at (1) quantifying the effects of spatial and temporal

[1]Department of Geography, University of Maryland, College Park, Maryland, USA.
[2]Climate Modeling and Diagnostics Laboratory, NOAA, Boulder, Colorado, USA.
[3]Altarum, Ann Arbor, Michigan, USA.
[4]Sukachev Forest Institute, Russian Academy of Sciences, Krasnoyarsk, Russia.
[5]Canadian Forest Service, Sault Ste. Marie, Ontario, Canada.

0886-6236/05/2004GB002300$12.00

variations in burned area, fuel density, depth of burning of surface organic layer fuels, and fire behavior/burn severity on trace gas emissions from boreal fires and (2) assessing the impacts of these emissions on atmospheric CO at several different temporal scales: seasonal, annual, and decadal. While the burned area in the boreal region is much lower than in tropical and subtropical regions, the amount of biomass consumed during fires can be significant because of the burning of large amounts of surface organic material present on top of mineral soil. Because of this and the fact that there are large interannual variations in burned area, wildland fire emissions can result in significant variations in atmospheric trace gas concentrations.

2. Background

[6] Approaches to estimate total carbon emissions (C_t) and emissions of a specific trace gas species (E_s) are based on the fundamental model introduced by *Seiler and Crutzen* [1980],

$$C_t = A \times B \times f_c \times \beta \quad (1)$$

$$E_s = C_t \times ef_s, \quad (2)$$

where A is the burned area (ha), B is the average density of the biomass (t ha^{-1}), f_c is the carbon fraction of the biomass, β is a scaling factor for the fraction of the biomass that is consumed (related to the type or intensity of the fire and the biomass being burned), and ef_s is the emission factor for a specific trace gas species, s (typically expressed as grams of the species per kilogram of dry matter consumed during the fire).

[7] In most vegetation types found outside of the boreal region, estimating emissions requires considering burning of aboveground live and dead vegetation as well as a shallow layer of litter (dead foliage and twigs lying on the ground surface). Many boreal forests and peatlands contain a deeper layer of organic matter that lies on top of the mineral soil (hereinafter referred to as the surface organic layer) which, in addition to litter, consists of lichen, live and dead moss, and organic soil (which has a very low mineral soil content and therefore can burn) [see, e.g., *Harden et al.*, 2004]. In addition, dead woody debris in the form of boles, branches, and roots may also be present in this surface organic layer. The fire science community refers to the surface organic layer as duff [*Miyanishi*, 2001; *Harden et al.*, 2004], which includes (1) upper duff consisting of the top layer of litter, lichen, live and dead moss, and a fibric layer (Canadian soil system) or Oi layer (U.S. soil system) and (2) lower or deep duff consisting of a highly decomposed mesic and/or humic soil layers (Canadian system) or Oe layer (U.S. System).

[8] In boreal regions, the depth of the surface organic layer varies from 4 to 10 cm in warmer, well-drained forests to 15 to >50 cm deep in forests underlain by permafrost, to 50 to >200 cm deep in peatlands. The depth to which the surface organic layer is consumed during fires is highly variable in both forests and peatlands. If sufficiently dry, the organic layer can ignite and burn and remove from 2 cm to well over 20 cm of organic material. The amount of carbon released during burning of surface organic layers in boreal forests and peatlands ranges between 2 and 15 t C ha^{-1}

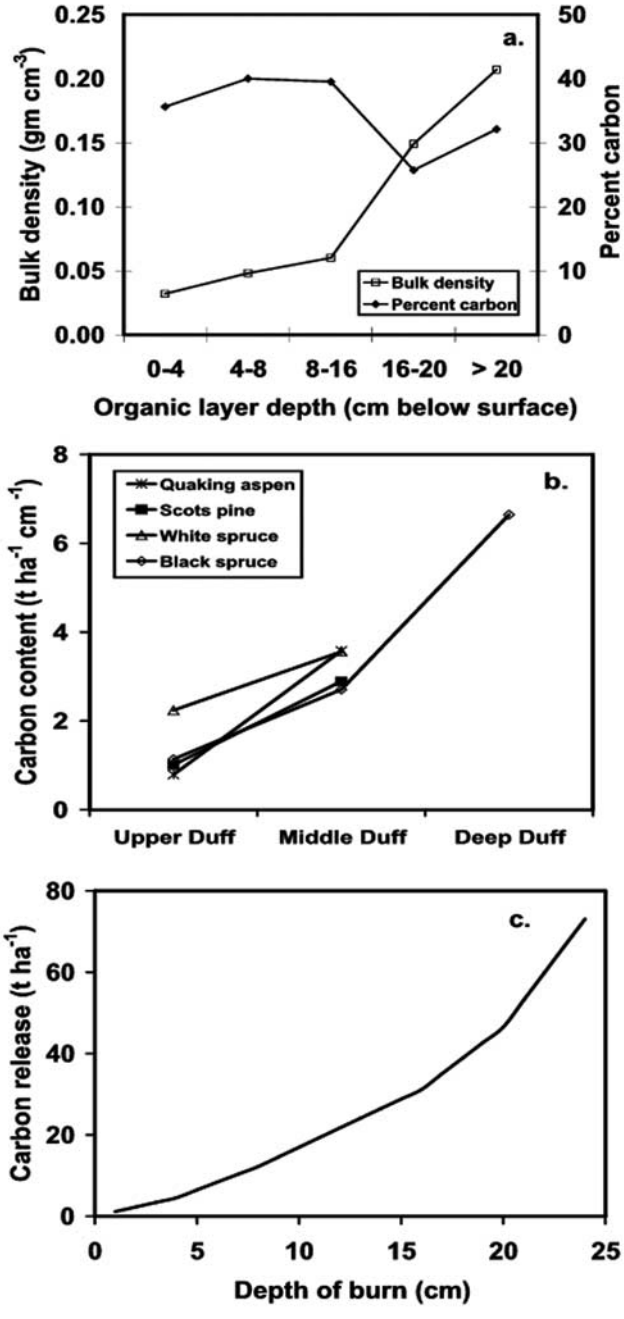

Figure 1. (a) Variations in bulk density and percent carbon as a function of depth of the organic mat from data collected in a black spruce forest [from *Kasischke et al.*, 2000]. (b) Comparison of variations in carbon content of the upper duff layers of boreal forests based on data from *Kasischke et al.* [2000] for black spruce, aspen, and white spruce forests, and from the *FIRESCAN Science Team* [1996] for the pine-lichen forest. (c) Variation in total carbon release from fires in the black spruce forest site in Figure 1a as a function of depth of burn.

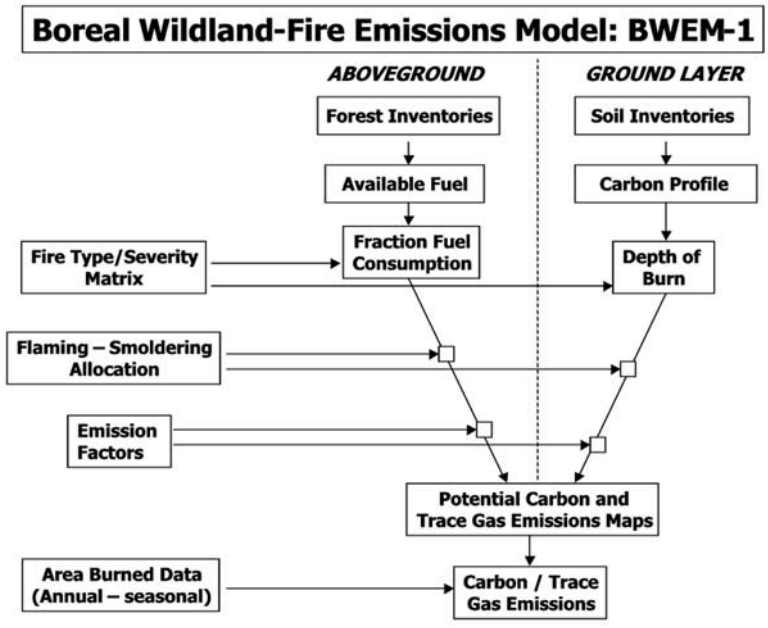

Figure 2. Flow diagram outlining the structure and organization of the Boreal Wildland-Fire Emissions Model (BWEM-1). For examples of the potential carbon emission maps as a function of the different fire severity scenarios, see auxiliary materials.

during lower intensity surface fires or where the depth of this layer is shallow [*Stocks and Kauffman*, 1997; *FIRESCAN Science Team*, 1996; *Benscoter and Wieder*, 2003; *McRae et al.*, 2005] to as high as 40 to >60 t C ha^{-1} during ground fires at sites with deeper and drier layers [*Kasischke et al.*, 2000; *Turetsky and Wieder*, 2001] (see also E. S. Kasischke and J. F. Johnstone, Variation in ground-layer surface fuel consumption and its effects on site characteristics in a black spruce forest complex in Interior Alaska, submitted to *Canadian Journal of Forest Research,* 2005) (hereinafter referred to as Kasischke and Johnstone, submitted manuscript, 2005).

[9] Estimating emissions from the burning of the organic mat requires not only determining the depth of burn, but accounting for variations in the carbon content of the different layers of the organic mat. The bulk density and carbon fraction of surface layer organic matter both vary with depth, with lower bulk densities and higher carbon fractions being found in the upper layers than in lower layers (Figure 1a). This characteristic means that the lower portions of the surface organic layer (deep duff) have a greater carbon mass per unit depth than the upper layers (shallow duff), primarily because of higher bulk densities. The carbon density for the black spruce forest represented in Figure 1a increases from 1.1 t C ha^{-1} cm^{-1} (11 kg C m^{-3}) in the uppermost layer (0–4 cm) to 6.6 t C ha^{-1} (66 kg C m^{-3}) in the deepest layer (> 20 cm) (Figure 1b). Variation in carbon density with depth is a characteristic common to all forest types found in the boreal region (Figure 1b), which means that the amount of carbon released increases nonlinearly as a function of the depth of burn (Figure 1c).

[10] Finally, burning of surface layer fuels affects the proportion of trace gas species emitted during fires, and in turn, the emission factors used in equation (2). While flaming combustion is common during the burning of aboveground vegetation in boreal systems, surface organic layer fuels (particularly organic peat and organic soils) are primarily consumed during smoldering combustion for three reasons: (1) The high packing ratios (ratio of the fuel volume to total volume of the fuel bed) result in insufficient oxygen to sustain flaming combustion [*Frandsen*, 1991], (2) the moisture content of the fuels reduces the overall temperature of combustion [*Miyanishi*, 2001], and (3) fuels in the surface organic layer have higher lignin content and release proportionally less of the volatile organics that result in flaming combustion [*Miyanishi*, 2001]. Both laboratory [*Yokelson et al.*, 1997] and field measurements [*Cofer et al.*, 1990, 1996a, 1996b, 1998] show that smoldering combustion releases a higher proportion of a number of important reduced trace gas (e.g., CO, CH_4) species than does flaming combustion because of lower combustion efficiencies.

3. Methods

[11] We estimated emissions from wildfires in the boreal regions of North America (BNA) (Canada and Alaska) and eastern Russia (BER) (Russia east of the Ural Mountains), and compared these to the average atmospheric CO in the high Northern Hemisphere (HNH) region (the extratropical, boreal, and arctic areas north of 30°N latitude) as measured from surface flask data obtained through the U.S. National Oceanic and Atmospheric Administration's Climate Modeling and Diagnostics Laboratory (CMDL) network (see supplemental Figure 1 in auxiliary material)[1]. We focused

[1] Auxiliary material is available at ftp://ftp.agu.org/apend/gb/2004GB002300.

Table 1. Summary of Depth of Burning and Total Carbon Present in the Top 5 cm of Ground-Layer Organic Matter in Different Boreal Forests

	Black Spruce[a]	White Spruce[a]	Aspen[a]	Black Spruce/ Sphagnum[b]	Black Spruce/ Feathermoss[b]	Pine/ Lichen[c]	Black Spruce/ Lichen[d]	Average	Standard Deviation
C in top 5 cm, t ha^{-1}	6.5	13.5	13.0	10.0	5.0	5.0	3.5	8.1	4.1
C density, t ha^{-1} cm^{-1}	1.3	2.7	2.6	2.0	1.0	1.0	0.7	1.6	0.8
Depth of burn, cm	6 to 24	7	5	n/a	n/a	8	n/a		

[a] *Kasischke et al.* [2000].
[b] *Harden et al.* [1997].
[c] *FIRESCAN Science Team* [1996].
[d] *Auclair* [1985].

on the years when burned area information derived from satellite data was available for the BER: 1992 and 1995–2003. Emissions from industrial sources and other wildland fires in other HNH regions were also estimated.

3.1. Estimating Emissions From Boreal Wildland Fires

[12] Figure 2 presents an outline of the overall approach to estimate total carbon and trace gas emissions from boreal wildland fires (named the Boreal Wildland-Fire Emissions Model or BWEM-1), which represents a refinement and extension of our previous methods [*Kasischke et al.*, 1995; *French et al.*, 2000, 2002; *Kasischke and Bruhwiler*, 2002]. In this approach, we considered aboveground and surface-layer biomass separately. We first generated a set of potential emissions maps to allow for estimation of emissions by combining these with area burned products using a geographic information system (GIS). The use of a GIS provided the flexibility to analyze different burn severity scenarios and to provide outputs in a variety of spatial/temporal formats.

[13] Estimating emissions from aboveground biomass (B_a) closely followed the original *Seiler and Crutzen* [1980] approach with the exception that we specified the fraction of aboveground biomass that is available to burn [$F_{b\text{-}a}$], and estimated emissions as a function time (t) during the fire season. On the basis of this modification, the potential carbon released from the burning of aboveground biomass is $C_{p\text{-}a}$ (t) estimated as

$$C_{p\text{-}a}(t) = B_a \times f_{c\text{-}a} \times F_{b\text{-}a} \times \beta_a(t), \quad (3)$$

where $\beta_a(t)$ is the fraction of the aboveground biomass that is consumed, and $f_{c\text{-}a}$ is the carbon fraction of aboveground biomass.

[14] For estimating potential emissions from the burning of the surface organic layer (denoted by the subscript g), we used a different approach. Here we determined the amount of carbon released from a fire based on the depth of burning of the surface organic layer (d_b). Potential carbon release from burning of the surface organic layer at different times of the growing season [$C_{p\text{-}g}$ (t)] can be estimated as

$$C_{p\text{-}g}(t) = C_g(d) d_b(t), \quad (4)$$

where $C_g(d)$ is the carbon density of the surface organic layer as a function of depth, d (Figure 1), and $d_b(t)$ varies as a function of seasonal differences in fire type and organic layer moisture.

[15] At this stage, we allocated the total carbon released from fires into flaming [$C_{pt\text{-}f}(t)$] and smoldering [$C_{pt\text{-}s}(t)$] components following the approach of *Kasischke and Bruhwiler* [2002],

$$C_{pt\text{-}f}(t) = D_a\, C_{p\text{-}a}(t) + D_g\, C_{p\text{-}g}(t) \quad (5)$$

$$C_{pt\text{-}s}(t) = S_a\, C_{p\text{-}a}(t) + S_g\, C_{p\text{-}g}(t), \quad (6)$$

where D is the fraction that occurs during flaming combustion and S is the fraction that occurs during smoldering combustion (where $S = 1 - D$). These potential carbon estimates (see supplemental Figure 2 in auxiliary material) are then multiplied by the appropriate emission factors using equation (2) to generate maps of potential trace gas emissions. Finally, the maps of potential emissions are combined with maps of burned area to calculate emissions during a specific time period. The approaches and rationale used to obtain the parameters in equations (2) to (6) are discussed in the following sections.

3.1.1. Spatial Distribution of Aboveground Carbon ($B_a \times f_{c\text{-}a}$)

[16] For the BNA region, we used biomass data from forest inventories for Canada developed by the Canadian Forest Service [*Lowe et al.*, 1996] and the spatial data set developed by *Kasischke et al.* [1995] for Alaska. For Russia, we used databases containing aboveground biomass information from *Alexyev et al.* [2000] (available from *Schlesinger and Stone* [2001]). The cell size of the BNA data was 0.5° by 0.5° and the BER data was 8 by 8 km. For aboveground biomass, we assumed $f_{c\text{-}a}$ was 45.

3.1.2. Spatial Distribution of Surface-Layer Carbon ($C_g(d)$)

[17] Spatial variations in surface-layer organic matter were determined using soil carbon databases available for Canada and Alaska from *Tarnocai* [1997] and *Lacelle et al.* [1997] and for Russia from *Stolbovoi and McCallum* [2002]. We assumed that only the fuel in the top 30 cm of organic soil was vulnerable to burn, and used the carbon density in this layer in our calculations. These soil databases were generated from large-scale soil maps (1:2,500,000) and had a cell size estimated to be 0.5° by 0.5°. On the basis of the data from a number of field studies, we assumed that the top 5 cm of all boreal forests

Table 2. Fraction of Available Aboveground Fuel Consumed During Fires

	Average Carbon in Aboveground Biomass		
	<10 t C ha^{-1}	10 to 20 t C ha^{-1}	>20 t C ha^{-1}
Surface fire	0.4	0.15	0.075
Crown fire	1	0.7	0.6

and peatlands surface organic layers had an average carbon density of 8.0 t C ha^{-1}, or 1.6 t C ha^{-1} cm^{-1} (Table 1). For the layers deeper than 10 cm below the surface, we estimated the average carbon density based upon the value reported in the soil carbon database for the top 30 cm. For depths between 5 and 10 cm, we assumed an average value between the shallow (0 to 5 cm) and deep (>10 cm) layers. This approach resulted in a profile where the average carbon density increased as function of depth as depicted in Figure 1.

3.1.3. Fraction of Aboveground Biomass Available to Burn ($F_{b\text{-}a}$)

[18] Aboveground biomass that burns during fires is usually restricted to foliage, small twigs, branches smaller than a certain size (usually <2 cm in diameter), and dead woody debris [*Stocks*, 1980, 1987, 1989; *Kasischke et al.*, 2000; *Shvidenko and Nilsson*, 2000]. As a general rule, shrubs have a higher fraction of biomass available for burning than trees, and as trees grow and increase in biomass, the proportion of biomass present in boles (trunks) and large branches increases [*Kasischke et al.*, 1994], resulting in a decrease in the proportion of fuel available for burning (branches, foliage) [*Kasischke et al.*, 2000]. To account for these variations, we assumed that (1) in areas where the total aboveground biomass was low (<10 t ha^{-1}), 80% of the aboveground biomass was available to burn; (2) where there were moderate levels of aboveground biomass (10 t ha^{-1} < average biomass <20 t ha^{-1}), 50% was available to burn; and (3) where there was high aboveground biomass (>20 t ha^{-1}), only 35% was available to burn.

3.1.4. Fractional Aboveground Fuel Consumption ($\beta_a(t)$)

[19] Variations in $\beta_a(t)$ were based on the combination of fire type, for example, surface or crown fire. In exercising the BWEM-1, fractional fuel consumption was assumed to be higher for crown than for surface fires (to reflect the higher energy state or intensity of crown fires) and decreased as the average aboveground biomass increased (to reflect the fact that as total biomass increases, the relative amount of fine fuel decreases). The fractional fuel consumption values in Table 2 are consistent with those for different forest types and biomass levels found in Alaska [*Kasischke et al.*, 2000], and produced average fuel consumption for aboveground vegetation consistent with observations from experimental fires [*FIRESCAN Science Team*, 1996; *Stocks and Kauffman*, 1997; *McRae et al.*, 2005]. The procedure used to determine $\beta_a(t)$ requires estimating the fraction of the area burned in surface and crown fires, which was assumed to vary as a function of time (season) and is discussed in the following section.

3.1.5. Determining the Fraction of Area Burned in Surface Versus Crown Fires

[20] Several generalizations can be made regarding fire types in the boreal forest region: (1) Surface fires are more prevalent in spring because after a sufficient period of drying after snowmelt, when fuel moisture conditions are low prior to the flushing of green vegetation. These conditions allow for the spread of surface fires. In early spring, temperatures are not high enough nor are relative humidities low enough to support crown fires in most regions. Once the surface vegetation layer begins to grow, the fuel moisture content of foliage increases, and lowers the occurrence of surface fires in many forest and vegetation types. (2) Large fire seasons occur because normal precipitation patterns (with increased rainfall beginning in late June to early July) fail to materialize due to variations in large-scale atmospheric circulation [*Skinner et al.*, 1999, 2002]. Because of this, crown fires become more prevalent in late season fires. (3) Crown fires are more prevalent in the North American boreal forest than in the Russian boreal forest because of differences in flammability of vegetation and trees found in the two regions, as well as the distribution of biomass in different sized fuels (e.g., boles, branches, twigs, foliage) [*Conard and Ivanova*, 1998]. (4) Most spring fires in Russia occur in the southern regions of the country where pine forests dominate [*Isaev et al.*, 2002]. Because surface fires are common to this forest type, we assumed that most early season fires in Russia were surface fires.

[21] An ongoing debate within the boreal forest fire community concerns the distribution of fires between surface and crown fires. Russian foresters believe surface fires are responsible for most (80%) of the burned area in BER during normal fire years [*Shvidenko and Nilsson*, 2000; *Conard and Ivanova*, 1998]. While surface fires are also common in the south-central portion of Siberia during summer fires [*Wirth et al.*, 1999; *McRae et al.*, 2005], analysis of SPOT VEGETATION satellite imagery of the large fires that occurred in Khabarovsk region during the middle and late parts of the growing seasons in 1998 showed that most of these fires were crown fires [*Kasischke and Bruhwiler.*, 2002; *Kasischke et al.*, 2003]. Analyses of AVHRR and Landsat imagery from other years indicate that a high percent of fires in Russia have satellite signatures that are characteristic of crown fires, particularly in eastern and northern forests dominated by larch (J. Hewson, personal communication, 2004).

Table 3. Fraction of Area in Surface Versus Crown Fires Assumed for Emissions Estimation[a]

	Early	Middle	Late
	Russia		
Crown	0.1	0.4	0.9
Surface	0.9	0.6	0.1
	North America		
Crown	0.7	0.8	0.9
Surface	0.3	0.2	0.1

[a]Early: through May for Russia, through June for North America; Middle, June/July for Russia, July for North America; Late: after July for Russia and North America.

Table 4. Depth of Burning (centimeters) of Ground Layer Organic Matter as a Function of Surface Versus Crown Fires and Time of Fire During the Growing Season Assumed for Emissions Estimation

	Early	Middle	Late
	Low Severity		
Surface	1.0	2.0	4.0
Crown	1.5	3.0	6.0
	Moderate Severity		
Surface	2.0	4.0	8.0
Crown	3.0	6.0	12.0
	High Severity		
Surface	2.0	4.0	8.0
Crown	3.0	6.0	13.0

[22] For BWEM-1, we assumed that more crown fires occurred in North America than in Russia, but that a higher proportion of burned area in Russia occurred during crown fires than other researchers assume [*Kajii et al.*, 2002; *Shvidenko and Nilsson*, 2000]. The fraction of burned area in surface versus crown fires were specified for three time periods, early, middle, and late, with the length of these periods being different for eastern Russia and North America (Table 3).

3.1.6. Depth of Surface Organic Layer Burning ($d_b(t)$)

[23] To estimate depth of burning, we assumed that (1) there was increased drying in the surface organic layer as the growing season progresses, resulting in deeper burning, especially during large fire years when precipitation levels are low; and (2) that deeper burns occurred during crown fires because of drier conditions. To implement these assumptions, we specified that crown fires burned 50% deeper than surface fires, and that the depth of burning doubled between early and middle and middle and late season fires (Table 4). Because there is no clear consensus on the depth of burning that occurs in boreal regions, we used three different burn severity scenarios, where the moderate scenario had twice the depth of burning as the low, and the high scenario included 1-cm-deeper burning during late season fires. A review of quick-look, Landsat satellite imagery from the large Russian fires that occurred in the spring (April/May) of 2003 indicates that a large portion of these fires were crown, not surface, fires. Because of this, for the high-severity scenario, we assumed that 40% of the spring fires in Russia in 2003 were crown fires.

3.1.7. Allocation Between Flaming and Smoldering Combustion (D_a, D_g, S_a, S_g)

[24] For this study, we assumed the same distribution of flaming/smoldering combustion for aboveground, vegetation biomass (80/20%) as used by *Kasischke and Bruhwiler* [2002]. For the surface layer, we assumed that flaming combustion only occurred during the burning of the top 2 cm of material (at a ratio of 30% flaming/70% smoldering), and that smoldering combustion was responsible for all burning in the deeper surface organic layers. This approach varies from that used by *Kasischke and Bruhwiler* [2002], who assumed a ratio of 20% flaming/80% smoldering for all surface-layer material. We believe this change is more consistent with the consensus within the fire science community that most surface organic layer burning occurs as smoldering combustion [*Frandsen*, 1991; *Miyanishi*, 2001].

3.1.8. Emission Factors for Flaming and Smoldering Combustion (ef_s)

[25] We used the average emission factors reported by *Kasischke and Bruhwiler* [2002] based on data collected by *Cofer et al.* [1990, 1996a, 1996b, 1998] and *Yokelson et al.* [1997].

3.1.9. Burned Area (A)

[26] To provide estimates of burned area for BER, we carried out analyses of AVHRR data collected over Russia during the years 1995 to 2003. Burned area estimates were derived by combining burn scar areas with areas estimated from mapping of hot spots [*Sukhinin et al.*, 2004]. This data set provided information on fire location and size on a daily basis. An ongoing study of the AVHRR hot spot information product for Russia that involves comparison with fire scars detected on Landsat imagery indicates that this product underestimates total burned area by 10 to 20% (J. Hewson, personal communication, 2004). For 1992, we used the total burned area estimates reported by *Cahoon et al.* [1996], who mapped fire scar boundaries from AVHRR data.

[27] For the Alaskan boreal forest, we obtained fire sizes and locations for all years from the large fire database maintained by the Alaskan Forest Service [*Kasischke et al.*, 2002]. For the Canadian boreal forest region, we used the large fire database developed by the Canadian Forest Service to establish locations of fires for the years 1992 and 1995 to 1999 [*Stocks et al.*, 2002]. For the year 2000 and beyond, burned area estimates were only available from the Canadian Forest Service at the provincial level (http://www.nofc.cfs.nrcan.gc.ca). To distribute the total burned area within the provinces, we used satellite data products to determine the location of large fires, including the FIRE M3 product (http://cwfis.cfs.nrcan.gc.ca/en/index_e.php) created by the Canadian Center for Remote Sensing [*Fraser et al.*, 2000] for years prior to 2000, and MODIS fire products (http://firemaps.geog.umd.edu/) for 2001 to 2003.

[28] Information on the temporal distribution of fires in Canada and Russia were obtained from information provided by thermal hot spot detection from AVHRR and MODIS imagery. For Alaska, temporal data were obtained from the National Interagency Coordination Center (NICC), which summarizes North American fire activity on a daily basis (http://www.cidi.org/wildfire). For this study, we aggregated the burned area data on a monthly basis for each year at a 1° by 1° grid spacing to combine with the potential emissions maps.

3.2. Peatland Burning

[29] We chose not to include a separate peatland category in BWEM-1 as has been done by others [see, e.g., *Shvidenko and Nilsson*, 2000; *Kajii et al.*, 2002; *Kasischke and Bruhwiler*, 2002; *Soja et al.*, 2004]. While up to 10–15% of the burned area in western Canada may be peatland [*Turetsky et al.*, 2004], this estimate was based on assuming that peatlands have an equal probability of burning as do uplands forests. No studies have actually

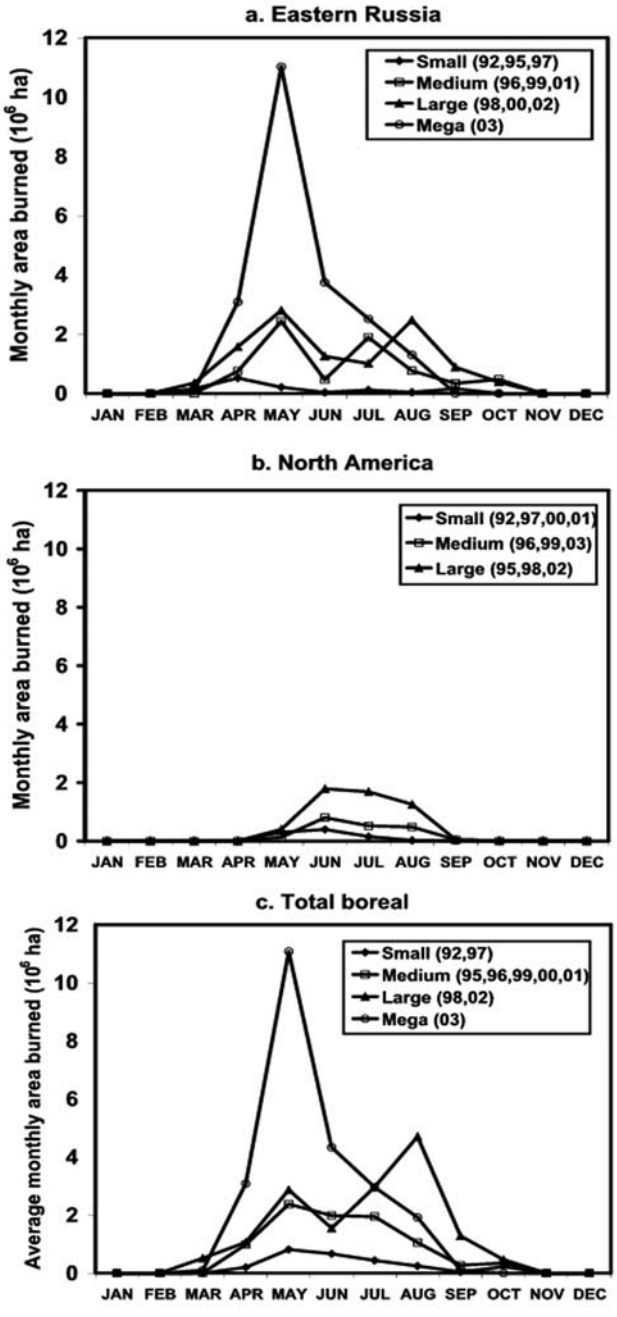

Figure 3. Monthly variations in average burned area for large and small fire years. Since 2003 was an unusually large fire year in Russia, we have called this a mega fire year.

quantified the differential rate of burning between uplands and peatlands at continental scales, and maps of the locations of peatlands are at coarse spatial scales that do not allow determining the degree to which peatlands actually burn. The depths to which peatlands burn during fires have not been measured to any great extent, and the limited studies that have been carried out [*Turetsky and Wieder*, 2001; *Benscoter and Wieder*, 2003; Kasischke and Johnstone, submitted manuscript, 2005] do not support an assumption that peatlands burn more readily (or deeper) than boreal forests with deep organic layers. Finally, the fact that peatlands have lower aboveground biomass and deeper surface organic layers than forests is reflected in the forest inventory/soil carbon databases used in this study.

3.3. Emissions From Nonboreal Wildland Fires in the HNH Region

[30] To estimate other sources of wildland fire emissions in the HNH region, we used average annual area burned statistics reported by national agencies and the United Nations [*Food and Agriculture Organization* (*FAO*), 1999] (also the NICC at http://www.cidi.org/wildfire/index.html; the Global Fire Monitoring Center at http://www.fire.uni-freiburg.de/welcome.html). Emissions were estimated for five additional regions within the HNH (supplemental Figure 1). For each region, we divided seasonal burned area data into three vegetation categories: forest, shrublands, and grasslands (steppe), and assumed that all emissions came from burning of aboveground biomass. We used data on average biomass levels and total carbon emissions for different temperate region vegetation types reported by *Leenhouts* [1998]. To estimate CO, we used the emissions factors reported by *Andreae and Merlet* [2001] for forest and *Leenhouts* [1998] for shrublands and grasslands.

3.4. Surface Carbon Monoxide Observations in the HNH Region

[31] The surface CO observations were generated from data collected by NOAA's Climate Modeling and Diagnostics Laboratory (CMDL), and are discussed in detail by *Novelli et al.* [2003]. For this study, we used the monthly average CO mixing ratio from observations collected at 15 stations located above 30°N latitude (the HNH region) (see supplemental Figure 1). We used observations from January 1991 through December 2003. From the average HNH CO mixing ratio estimates, we calculated the residual mixing ratio derived by subtracting the quadratic long-term trend and average seasonal cycle from the average mixing ratio derived from the flask samples.

3.5. CO Emissions From Industrial/Transportation Sources in the HNH Region Hemisphere

[32] We estimated CO emissions from industrial and transportation sources in the developed countries of the HNH region (including United States, Canada, western Europe, eastern Europe, Russia, and Japan) plus China from data reported by (1) the International Geosphere Biosphere Program's Global Emissions Inventory (http://arch.rivm.nl/env/int/coredata/geia/index.html), (2) the U.S. Environmental Protection Agency (http://www.epa.gov/air/aqtrnd99/PDF%20Files/tables/a_2.pdf), (3) the Program for Monitoring and Evaluation of Air Pollutants in Europe (EMEP) (http://www.emep.int), and (4) the Emission Database for Global Atmospheric Research (EDGAR) database (http://arch.rivm.nl/env/int/coredata/edgar/intro.html).

4. Results and Discussion

[33] For the time periods used in this study (1992, 1995–2003), there were large interannual variations in burned area

Table 5. Summary of Total Carbon and CO Emissions From Boreal Wildland Fires

	Carbon Emissions, Tg yr^{-1}			CO Emissions, Tg yr^{-1}		
	Low Severity	Moderate Severity	High Severity	Low Severity	Moderate Severity	High Severity
1992	21.2	33.5	38.5	6.4	11.9	14.0
1995	77.7	123.1	140.9	24.3	44.7	52.5
1996	70.1	104.3	115.4	21.5	36.8	41.6
1997	23.5	39.9	46.4	7.8	15.2	18.0
1998	211.6	348.3	421.8	68.6	130.9	163.3
1999	80.2	121.4	134.9	24.9	43.2	49.1
2000	82.4	124.9	137.5	25.6	44.5	49.9
2001	112.2	194.6	239.2	36.5	74.1	93.7
2002	193.2	317.5	381.8	62.0	118.4	146.5
2003	187.2	280.5	428.7	55.0	89.7	139.0
Average	105.9	168.8	208.5	33.2	60.9	76.8

in both BNA (0.8 to 7.3 $\times$ 10^6 ha yr^{-1}) and BER (0.9 to 21.7 $\times$ 10^6 ha yr^{-1}). Of the total burned area, 77% occurred in BER and 23% in BNA, with much variation between individual years. In 1995, 92% of the burned area occurred in BNA, while in 2003, 92% occurred in BER. Because of this variability, there was little correlation between burned area from the two regions ($r^2 = 0.02$, $p = 0.69$), indicating that the large-scale atmospheric circulation patterns controlling fire weather in these two regions are not linked.

[34] The seasonal patterns of burning varied between BER and BNA, with the fire season being longer in BER. During the three largest fire years (1998, 2002, and 2003), 52% of the total burned area occurred, and the seasonal patterns of burning were different during large and small fire years (Figure 3). There were an unusually large number of spring fires in Russia in 2003, which resulted the highest level of fire activity during April through June in BER. In the two other large fire years (1998 and 2002), the highest fire activity occurred later in the summer (July–September), with high fire activity in May as well. During the smaller years, the peak activity occurred during May–July (Figure 3a). In North America, fire activity peaked in June, and was only slightly lower in July and August during large fire years. At a global scale, the three largest fire years (2003, 1998, and 2002) had distinct seasonal patterns, with an early-season peak in May in 2003 and a late-season peak in August in both 1998 and 2002.

[35] Using the spatial information on potential carbon emissions and burned area, we are able to generate a wide variety of data products for use by atmospheric researchers and other interested scientists (see supplemental Figures 3 and 4 in auxiliary material). Here we present estimates of annual carbon emissions (section 4.1) and monthly and annual estimates of CO emissions (section 4.2).

4.1. Total Carbon Emissions From Boreal and Other High Northern Hemisphere Fires

[36] Our estimates of total carbon emissions from boreal fires ranged between 21 to 212 Tg C yr^{-1} for the low emissions scenario, 34 to 348 Tg C yr^{-1} for the moderate emissions scenario, and 38 to 429 Tg C yr^{-1} for the high emissions scenario (Table 5). Fires in the boreal region of eastern Russia (BER) accounted for 75% of the total boreal biomass burning emissions. However, in some years, fires in boreal North American (BNA) produced a significant portion of emissions, representing 43% of total emissions in 1997 and 91% in 1995.

[37] While the interannual variations in emissions are strongly correlated with annual area burned, a significant portion of variation was due to seasonal variations in fire activity, and differences in biomass and soil carbon densities in the regions where fires occurred. Average emissions (per unit area burned) for both BER and BNA varied by nearly a factor of 2 between different years (Table 6). Overall, the average emissions for fires in the boreal region were higher in Russia than in North America, mainly because of higher aboveground biomass levels as well as deeper organic soil layers.

[38] A significant portion of fire emissions in the boreal forest region originated from the burning of surface-layer organic matter, depending on the fire severity assumptions. Burning of surface-layer organic matter contributed 41% of the emissions BER and 48% in BNA using the assumptions of the low emissions scenario. These percentages increased to 63% (BER) and 69% (BNA) using the assumptions of the moderate emissions scenario and to 69% (BER) and 73% (BNA) with those of the high emissions scenario.

[39] We estimated that 9.4.$\times$ 10^6 ha yr^{-1} of forests, shrublands, and grasslands (steppe) burned each year in HNH regions outside of BER and BNA, releasing an average of 57.0 Tg C yr^{-1} (see supplemental Table 1 in auxiliary material). On average, HNH wildland fires result in 166 to 266 Tg yr^{-1} in total carbon emissions, with boreal fires producing 65% (low emissions scenario) to 79% (high emissions scenario) of the total.

[40] Our estimates of total carbon emissions from boreal fires were in some cases less than those estimated by other researchers in recent studies and overlapped those of others (Table 7). Our estimates were lower than those of *Andreae and Merlet* [2001] and *Soja et al.* [2004]. The reason for our differences with *Andreae and Merlet* [2001] are difficult to determine because they do not report any information on the burned area. Our estimates were lower than those from *Soja et al.* [2004] because they assumed a significant amount of peatland fire with deep burning of the surface organic layer, a higher proportion of crown fires, and deeper burning of the surface organic layer. Our moderate and high severity

Table 6. Summary of Average Emissions (t C ha^{-1}) From Wildland Fires in the Boreal Region

	Boreal Eastern Russia			Boreal North America		
	Low Severity	Moderate Severity	High Severity	Low Severity	Moderate Severity	High Severity
1992	9.0	14.8	17.5	8.8	13.0	14.0
1995	11.0	18.1	21.8	9.7	15.2	17.4
1996	9.1	13.3	14.6	9.3	14.6	16.5
1997	9.0	14.8	17.5	7.3	13.0	14.8
1998	14.4	23.1	28.0	12.0	21.1	25.6
1999	8.1	12.0	13.1	10.5	17.1	19.8
2000	7.4	11.1	12.2	10.8	17.5	19.8
2001	12.4	21.6	26.7	7.3	11.4	12.4
2002	13.6	22.3	27.2	9.1	15.2	17.3
2003	7.7	11.3	17.7	11.2	19.7	23.9
Average	10.2	16.2	19.6	9.6	15.8	18.1

Table 7. Comparison of Boreal Wildland Fire Emission Estimates[a]

		Total, Tg yr^{-1}				t ha^{-1} Burned			
	Area Burned, 10^6 ha	Average	Low	Moderate	High	Average	Low	Moderate	High
				Carbon Emissions					
Average HNH									
This study			162.9	225.8	265.5				
Andreae and Merlet [2001]	n/a	288.0							
HNH - 1997–2001									
This study			159.0	222.8	253.0				
Van der Werf et al. [2004]	n/a	140.0							
BER 1998									
This Study	10.8		155.5	249.1	304.9		14.4	23.1	28.2
Kajii et al. [2002]	9.9	175.5				18.8			
BER 1998–2002									
This study	9.6		110.3	177.9	212.2		11.5	18.6	22.2
Soja et al. [2004]	9.1		152.6	252.6	412.8		16.8	27.8	43.1
Canada 1995–1998									
This study	3.2		35.3	58.2	64.1		11.0	18.2	20.0
Amiro et al. [2001]	3.2	46.2				14.4			
				CO Emissions					
Average HNH									
This study			33.2	60.9	76.8				
Andreae and Merlet [2001]	n/a	68.0							
BER and BNA 1997–2001									
This study			32.7	61.6	74.8				
Van der Werf et al. [2004]	n/a	31.0							
BER 1998									
This Study	10.8		49.5	92.2	115.3		4.6	8.6	10.7
Kajii et al. [2002]	9.9	50.0				5.1			
BER 1998–2002									
This study	9.6		35.0	65.7	80.7		3.7	6.9	8.4
Soja et al. [2004]	9.1			62.6	103.6			6.9	10.8

[a]Entry n/a: not available.

scenarios produced higher emissions estimates than those from *Amiro et al.* [2001], *Kajii et al.* [2002], and *Van der Werf et al.* [2004] because BWEM-1 assumed a higher amount of crown fire (compared to *Kajii et al.* [2002]) and deeper burning of the surface organic layer (all studies). In addition, the BWEM-1 model produced higher estimates of emissions from burning of aboveground vegetation than the *Amiro et al.* [2001] approach (5.1 versus 2.0 t C ha^{-1}).

4.2. CO Emissions From Boreal and Other High Northern Hemisphere Fires

[41] We estimated that depending upon seasonal area burned, boreal fires produced from 6 to 69 Tg CO yr^{-1} using the assumptions of the low emissions scenario, 12 to 131 Tg yr^{-1} (moderate emissions scenario), and 14 to 163 Tg CO yr^{-1} (high emissions scenario) (Table 5). CO emissions from BER fires accounted for 75% of all boreal wildland fire emissions. When we used the single emissions factor of *Andreae and Merlet* [2001], the estimates were 33% (low emissions) to 52% (high emissions) lower than those from BWEM-1 because the single emission factor used by *Andreae and Merlet* [2001] did not account for smoldering combustion.

[42] With other HNH wildland fires generating 16.9 Tg CO yr^{-1} of emissions, total average HNH wildland fire CO emissions were 50 to 94 Tg yr^{-1}, with boreal fires producing from 66% (low emissions scenario) to 82% (high emissions scenario) of the total. The BWEM-1 estimates are higher than those by *Andreae and Merlet* [2001], *Kajii et al.* [2002], and *Van der Werf et al.* [2004], and span those of *Soja et al.* [2004] (Table 7). The higher CO emissions are partially due to using different emission factors to account for smoldering combustion.

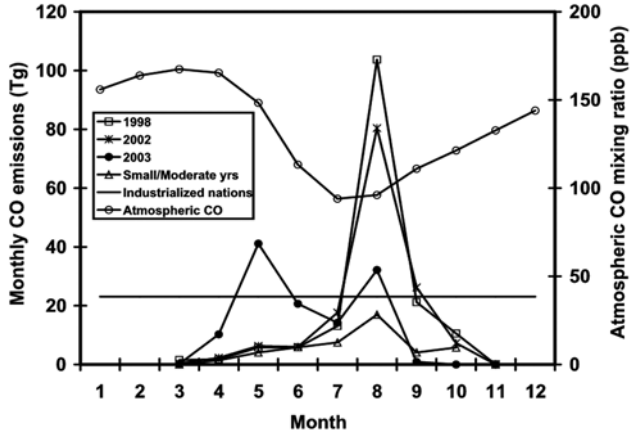

Figure 4. Seasonal patterns in boreal fire CO emissions for the moderate emissions scenario. Also presented in this plot is the average monthly HNH CO mixing ratios for the years 1991–2003 and the estimated average CO emissions from industrialized nations plus China for the period 1998–2003.

Table 8. Summary of CO Emissions From Industrial and Transportation Sources in the HNH Region (Tg yr^{-1})

	1991	1999
Industrialized nations	269	215
China	79	84
Total HNH	348	299

[43] Carbon monoxide (CO) is important in regulating air quality because it is a major sink for the hydroxyl radical (OH) which controls the oxidizing capacity of the troposphere [*Thompson*, 1992], and also can influence the production of other trace gas species (including ozone) which influence the chemistry and radiative forcing of the atmosphere [*Daniel and Solomon*, 1998]. Decreases in HNH CO observed from surface flask data during the early 1990s (1.5 ppb yr^{-1}) are attributed to reductions in industrial emissions in developed nations (United States, Canada, Western Europe, Eastern Europe, Russia, and Japan) [*Bradley et al.*, 1999; *Novelli et al.*, 2003].

[44] While CO emissions from HNH industrialized nations fell during the 1990s (Table 8), according to the EDGAR database, emissions from China were growing at a rate of 0.54 Tg CO yr^{-1}. Overall, there was a drop of 49 Tg yr^{-1} in industrial/transportation sector CO emissions in the HNH region over the 1990s. Assuming that the decrease in industrial/transportation CO emissions was linear, we estimated that during the period of 1998 to 2003, industrial/transportation emissions averaged 291 Tg CO yr^{-1} compared to 45 to 107 Tg CO yr^{-1} from boreal fires (16 to 37% of industrial emissions). During the three large fire years of 1998, 2002, and 2003, boreal fire emissions were 21 to 52% of annual industrial emissions. Because industrial/transportation CO emissions do not fluctuate during the year, on a monthly timescale, boreal fire emissions may approach and exceed these emissions during years experiencing high levels of biomass burning, such as 1998, 2002, and 2003 (Figure 4). During other years, boreal fire emissions are usually much lower than industrial emissions. The effects of seasonal variations in boreal fire emissions are discussed in the following section.

4.3. Effects of Boreal Fire Emissions on Atmospheric CO

[45] The average CO mixing ratio for all the stations located in the HNH region exhibits variability at multiple timescales (Figure 5). CO emissions from industrial and transportation sources in the HNH region are thought to be fairly constant throughout the year; thus, in the absence of biomass burning, the seasonal variations observed in the HNH CO mixing ratio are due to variations in the reduction capacity of the atmosphere based upon seasonal variations in the concentration of the OH radical combined with oxidation rates of methane (CH_4), which also depends on the OH radical. On average, from 1991 to 2003 the atmospheric CO concentration reached its annual maximum in late March and its annual minimum in late July (Figure 4).

[46] Variations in the atmospheric CO mixing ratio for the individual years of 1992 and 1998 are compared to the average seasonal CO mixing ratio in the left-hand column of Figure 6 (plots for all years are presented in Figure 5 of the auxiliary material), and the CO mixing ratio residual are

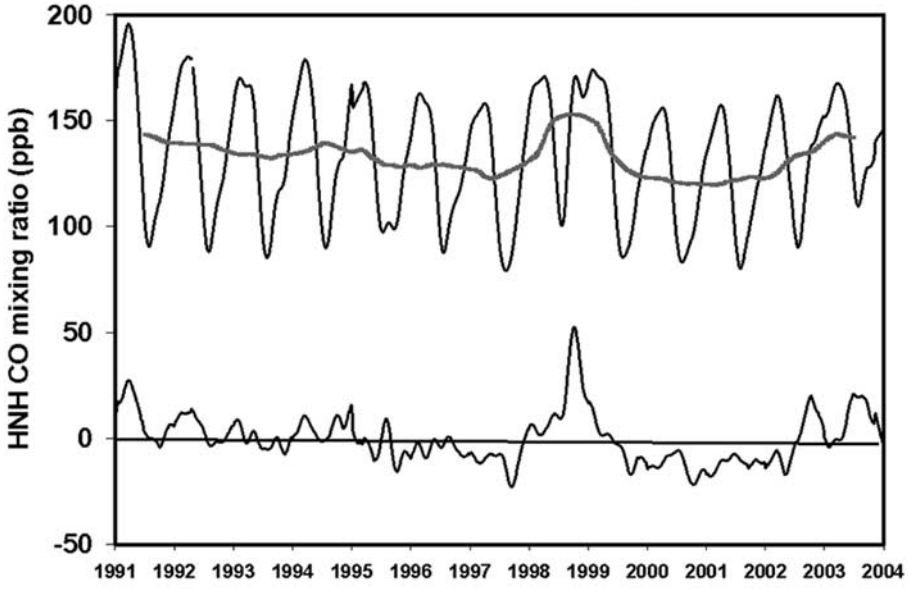

Figure 5. (top) Average CO mixing ratio for the period of 1991 to 2003 based on the average of measurements collected at 17 stations in the HNH region, and (bottom) the residual of the mixing ratio (bottom plot). The shaded line in the top plot represents a 1-year running average of the HNH CO mixing ratio.

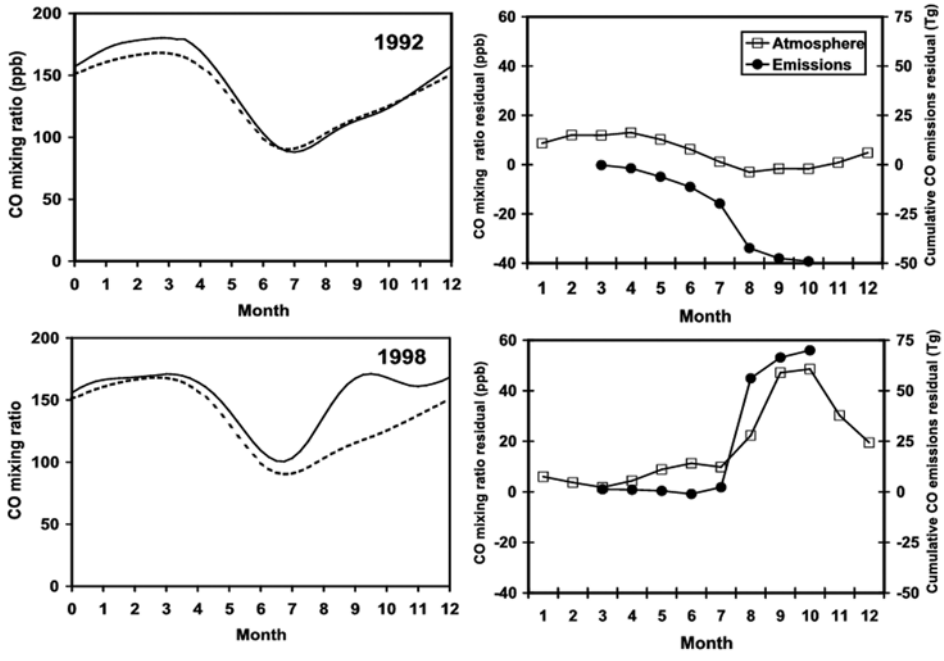

Figure 6. (left) Comparison of the average HNH CO mixing ratio (dashed line) to the HNH mixing ratio residual observed in 1992 and 1998 (solid line). (right) Comparison of the HNH CO mixing ratio residual to the cumulative boreal fire emissions CO residual generated from the moderate emissions scenario. The plots for the remaining years can be found in supplemental Figure 5 of the supplemental material.

compared to the cumulative CO emissions residual using the moderate emissions scenario in the right-hand column. CO boreal fire emissions residuals were calculated by taking the monthly profile of CO emissions for all years and subtracting it from the monthly CO emissions estimates. For best comparison to the CO mixing ratio residual, the excess CO burden was approximated by the cumulative CO emissions residuals from the start of the fire season. Plots using the low and high emissions scenario estimates and burned area resulted in trends similar to those presented in Figure 6.

[47] There were statistically significant linear correlations between the CO mixing ratio residuals and the cumulative CO emissions residuals in 8 out of the 10 years (Table 9). On average, the moderate scenario CO emissions accounted for the highest proportion of the variation in the seasonal CO mixing ratio (average $r^2 = 0.64$), but was closely followed by the low and high emissions scenario residuals (average $r^2 = 0.63$). The burned area residuals accounted for the lowest proportion of the variation in the seasonal atmospheric CO mixing ratio (average $r^2 = 0.57$).

[48] In the three years with the greatest fire activity (1998, 2002, and 2003), the correlation between the increasing atmospheric CO mixing ratio and the large boreal fire emissions was readily detected. For 1998 and 2002, the sharp rises in the late season atmospheric CO residual corresponded to the large increases in the CO emissions residual (Figure 6). For 2003, the atmospheric CO experienced a sharp increase in late May and early June, a rise that corresponds to the emissions residual resulting from the large springtime fires occurring that year. The decrease in the late-season CO mixing ratio in 2003 was matched by a decrease in the CO emissions residual.

[49] In the 2 years with the lowest fire activity (1992 and 1997), there was a decrease in the CO mixing ratio residual that correlates with the decreasing CO emissions residual that occurred during these years (Figure 6). While the linear correlation between the CO mixing ratio and CO emissions is much lower in 1995 than in other years, a closer examination showed that the increase in atmospheric CO in the middle of the fire season does corresponded to the

Table 9. Summary of Linear Correlation Coefficients $(r^2)^+$ Between Atmospheric CO Residual and Cumulative Emissions and Area Burned Residuals for the Specific Years Used in This Study

	Low Emissions	Moderate Emissions	High Emissions	Area Burned
1992	0.93[a]	0.89[a]	0.87[a]	0.95[a]
1995	0.39	0.42[b]	0.39[b]	0.24
1996	0.03	0.03	0.06	0.08
1997	0.59[b]	0.63[b]	0.62[b]	0.36
1998	0.86[a]	0.87[a]	0.86[a]	0.82[a]
1999	0.86[a]	0.87[a]	0.89[a]	0.74[c]
2000	0.70[c]	0.69[c]	0.61[b]	0.60[b]
2001	0.18	0.20	0.23	0.22
2002	0.91[a]	0.90[a]	0.89[a]	0.92[a]
2003	0.88[a]	0.92[a]	0.85[a]	0.79[a]

[a]Values statistically significant at $p < 0.001$.
[b]Values statistically significant at $p < 0.1$.
[c]Values statistically significant at $p < 0.01$.

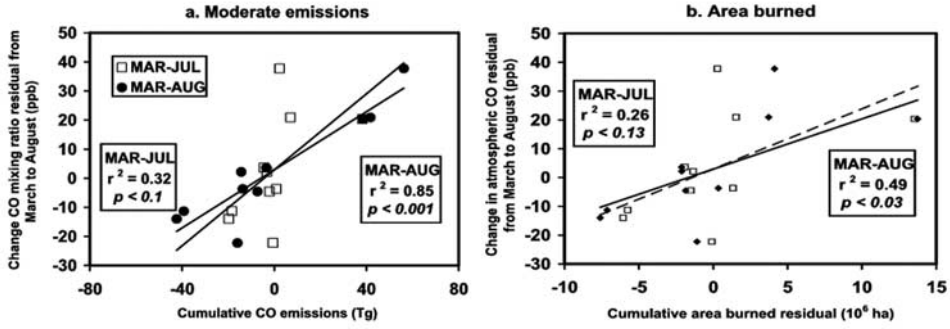

Figure 7. Plots of the changes in the atmospheric CO residual between March and August for all years (1992 and 1995 to 2003) as a function of (a) the cumulative CO emissions residuals for March to July and March to August and (b) the cumulative area burned residuals for March to July and March to August. This plot was generated using estimates generated using the moderate severity scenario.

large fires that occurred in western Canada during this year, where 5.6×10^6 ha of fire occurred in June and early July. The lack of correlation between atmospheric CO and boreal fire emissions in 1996 and 2001 is most likely due to the occurrence of large fires in other parts of the Northern Hemisphere during these years (there were 2.5×10^6 ha of wildland fire in the conterminous United States during 2001 and 10.1×10^6 ha of wildland in the steppes and forests of Mongolia during 1996). This latter observation demonstrates the need to better quantify wildland fire emissions from other HNH regions on a seasonal basis.

[50] In a repeat of the analysis of *Wotawa et al.* [2001], using simple linear correlation, we found that interannual variations in burned area in BER Russia accounted for 36% of the variation in the average CO mixing ratio in July and August, while variations in burned area in BNA accounted for 22%. Using multiple-linear correlation, we found that the areas burned in Russia and North America accounted for 69% of the variation in the average July/August CO mixing ratio, which was slightly higher than the 63% found by *Wotawa et al.* [2001].

[51] In addition to above correlation analyses, we calculated the linear correlation between the interannual variations in seasonal changes in the CO mixing ratio residual and the cumulative burned area residual or CO emissions residual for specific time periods during the fire season (ranging from March to May to March to October). This analysis was used to test two hypotheses. First, we hypothesized that interannual variations in changes in atmospheric CO during specific time periods during the summer were the result of interannual variations in boreal fire emissions. Second, we hypothesized that because of differences in fire types and emissions densities, variations in estimated emissions would explain more of the variability in atmospheric CO than variations in burned area.

[52] Figure 7a presents a plot of changes in the average monthly CO mixing ratio between March and August as a function of the cumulative CO emissions residual from March to July and March to August using estimates from the moderate emissions scenario. This plot shows that the interannual variations in emissions from boreal fires between March and August explained 85% of the variations in the atmospheric CO residual from March to August, while emissions from fires between March and July only explained 32%. The trends in this plot support the first hypothesis presented above. We can see that years with large positive emissions residuals (e.g., years with high emissions) corresponded to years with large increases in atmospheric CO, while years with negative emissions residuals (e.g., years with low emissions) corresponded to years with decreases in atmospheric CO. Figure 7b presents a plot of changes in the average monthly CO mixing ratio between March and August as a function of the cumulative burned area residuals. From this plot, we can see that burned area explained a lower portion of the overall variation in the atmospheric CO residuals (particularly for the March to August changes), supporting the second hypothesis presented above.

[53] Figure 8 presents a plot of the correlation coefficients between cumulative CO emissions from the moderate emissions scenario for different time periods ranging from

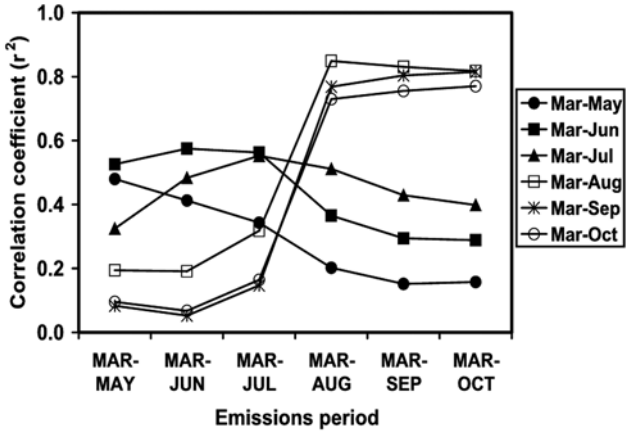

Figure 8. Correlations between the cumulative CO emissions residual for specific time periods and changes in the HNH CO mixing ratio residual for specific time periods. This plot was generated using estimates generated using the moderate severity scenario.

March to May to March to October and changes to the atmospheric CO residual for different time periods, ranging again from March to May and March to October. This plot shows that the early season boreal fire emissions explained most of the variation in changes in the early season atmospheric residuals, but that over the entire fire season, it is the season-long emissions that explained most of the variation in atmospheric CO. The trends in the plots for the low and high emissions scenario CO and area burned were very similar to those presented in Figure 8, where the average correlation (r^2) for the March to August through March to October time periods was 0.79 for the moderate emissions scenario, 0.77 for the high emissions scenario, 0.75 for the low emissions scenario, and 0.41 for area burned. Finally, using emissions from North America and Russia as independent variables in a multiple-linear correlation model did not increase the statistical correlation.

[54] Over the longer term, variations in emissions from industrial and transportation sources in the Northern Hemisphere industrial nations have contributed to levels of atmospheric CO. *Zander et al.* [1989] concluded that increases in CO observed over the Swiss Alps between the 1950s and 1990s were due to industrial emissions from Europe. Decreases in the HNH CO mixing ratio observed during the 1980s and early 1990s were attributed to the reductions in CO emissions from Northern Hemisphere industrialized nations as a direct result of pollution control efforts (Table 8) combined with increases in atmospheric OH [*Bawkin et al.*, 1994: *Khalil and Rasmussen*, 1994; *Novelli et al.*, 1994]. Between 1991 and 1997, the average HNH CO averaged over the entire year experienced a 3.3 ppb decrease; however, this downward trend was dramatically reversed in 1998 by emissions from large fires in the boreal regions combined with the transport of CO from fires in Southeast Asia and Central America into the Northern Hemisphere [*Van der Werf et al.*, 2004; *Yurganov et al.*, 2004]. The average HNH mixing ratio in 1998 was higher than in 1991 (151.5 ppb in 1998 versus 143.4 ppb in 1991). After 1998, the average HNH mixing ratio continued to decrease for 2 years, but then increased over the next 3 years (2001–2003) by an average of 7.1 ppb yr^{-1} (Figure 5). This increase in HNH CO corresponds to 3 years where boreal fire emissions were substantially above those during the early 1990s. We estimate that boreal fire CO emissions from the 1998 to 2003 time period were 27 to 68 Tg yr^{-1} higher than they were during the 1992 to 1997 time period (assuming that 1993 and 1994 were moderate fire years in Russia). This increase in boreal fire emissions far exceeds the rate of decrease in CO emissions estimated for the HNH industrialized nations for the period of 1990 to 1999 (6 Tg CO yr^{-1}). Thus, in addition to explaining interseasonal and intraseasonal variations in HNH CO, the substantial increase in fire activity during the late 1990s/early 2000s appears to have had a significant impact on longer-term trends.

5. Conclusions

[55] Studies have shown that the large fire events during the 1997/1998 time period in Southeast Asia, Central and South America, and the Northern Hemisphere boreal region were responsible for a significant portion of the observed interannual variation in atmospheric CO, CO_2, and CH_4 [*Dlugokencky et al.*, 2001; *Wotawa et al.*, 2001; *Langenfelds et al.*, 2002; *Duncan et al.*, 2003a; *Novelli et al.*, 2003; *Van der Werf et al.*, 2004]. At regional scales, these fires have been shown to impact atmospheric CO concentration in the HNH region as well [*Forster et al.*, 2001; *Kondo et al.*, 2003; *Matsueda and Inoue*, 1999; *Duncan et al.*, 2003b; *Kasischke and Bruhwiler*, 2002; *Yurganov et al.*, 2004]. In this study, we found that interannual variations in wildland fire CO emissions in the boreal region were controlled by a variety of factors, not just area burned. Using the BWEM-1 model to generate emissions, we demonstrated that the impact of boreal wildland fires on atmospheric CO extends beyond the large fire year of 1998.

5.1. Controls on Emissions From Wildland Fires in the Boreal Region

[56] In this study, we implemented a new method to quantify levels of emissions from fires in the boreal region. We used standard approaches to estimate carbon release from burning of aboveground vegetation, where biomass maps derived from forest inventory maps were used to describe the spatial variations in fuel loads, and seasonal variations in fire types (crown versus surface) were used to specify fraction of biomass consumed. However, we developed a new approach to estimate carbon released during the burning of surface layer organic matter that varied depth of burn between different fire types and times of the year, and accounted for variations in carbon density in the surface layer (Figure 1).

[57] We found that while there were large interannual variations in emissions driven by differences in area burned, the location of the fires relative to the availability of fuels and the timing of the fires during the growing season also influenced emissions. In particular, on the basis of the assumptions regarding the mixture of surface and crown fires and depth of burning as a function of timing of the fire during the growing season, fires occurring later in the growing season resulted in significantly greater emissions than those occurring earlier in the growing season. As a result, there were large year-to-year variations in average carbon and trace gas emissions from fires (Table 6). By accounting for the spatial and temporal variations in fuel load and biomass consumption, we were able to account for a higher percent of variations in atmospheric CO than through using area burned information alone (Table 9).

5.2. Effects of Boreal Wildland Fire Emissions on Atmospheric CO

[58] The results from this study showed that emissions from wildland fires in the BER and BNA regions affect atmospheric CO concentrations in the HNH region at multiple temporal scales. On a seasonal basis, boreal wildland fire emissions occur at a time when the concentration of HNH CO is decreasing and is approaching its annual minimum (Figure 4). The level of wildland fire emissions during the growing season can be greater than those originating from industrial emissions, and the timing of these emissions can influence seasonal HNH CO levels

(Figure 4). Interannual variations in boreal wildland fire emissions also explain a statistically significant portion of the interannual variations in HNH CO (Figures 7 and 8). Finally, the increases in average HNH CO in 1998 and between 2001 and 2003 may be the direct result of high levels of boreal fire activity during these periods.

5.3. Future Research Needs

[59] A number of recent studies have developed estimates of emissions from fires in the boreal region. The primary difference in the estimates from these studies lies in two areas: (1) assumptions regarding the type of fires that occur in the boreal region and (2) estimating the amount of burning that occurs in the surface organic layer, in particular in peatlands and forests underlain by permafrost. A modeling study by *French et al.* [2004] indicated that parameterization of surface organic layer burning is the largest source of uncertainty in boreal wildland fire emissions.

[60] To address these uncertainties, research is need in the following areas: (1) More studies of the type carried out by *Turetsky et al.* [2004] are needed, where maps of peatland types derived from aerial photography are compared with perimeter maps for specific fire events. Field surveys are also needed to determine the types of fires that occur in peatlands, for example, surface fires that burn only the vegetation versus ground fires that consume layers of carbon-rich peat.

[61] (2) The importance of quantifying the patterns of surface fuel consumption (SFC) in boreal regions was illustrated in this study. Increasing the depth of burn by 1 cm for late season in the high emissions scenario increased total carbon emissions by 19%. Field-based studies need to be carried out to better quantify the levels of GFC that occur in boreal areas with deep organic mats. To more accurately account for variations in SFC in emissions estimates, models need to be developed to quantify the factors that control SFC. (3) The levels of emissions are also controlled by assumptions related to type of fire in different boreal regions, with much higher emissions occurring in crown versus surface fires. The differences in emissions between the moderate and high scenario were partially due to changing the assumptions regarding the types of fires that occurred in Russia in 2003. The damage inflicted on the vegetation of a site is very dependent on the type of fire, and can easily be determined via analyses of satellite imagery [see, e.g., *Michalek et al.*, 2000; *Isaev et al.*, 2002]. Thus research should be carried out to assess variations in fire type in different boreal regions using satellite imagery.

[62] **Acknowledgments.** The support for this research at the University of Maryland was provided through the National Aeronautics and Space Administration through grant NAG-59440 and Fellowship NGT-530377. We would like to thank the MODIS Fire Product team (in particular, Chris Justice) for providing access to active fire products for Canada and Alaska. The authors would like to thank the two anonymous reviewers for their helpful comments and suggestions.

References

Alexyev, V. A., R. A. Birdsey, V. D. Stakanov, and I. A. Korotkov (2000), Carbon storage in the Asian boreal forests of Russia, in *Fire, Climate Change, and Carbon Cycling in the Boreal Forest*, edited by E. S. Kasischke and B. J. Stocks, pp. 239–257, Springer, New York.

Amiro, B. D., J. B. Todd, B. M. Wotton, K. A. Logan, M. D. Flannigan, B. J. Stocks, J. A. Mason, D. L. Martell, and K. G. Hirsch (2001), Direct carbon emissions from Canadian forest fires, 1959–1999, *Can J. For. Res.*, *31*, 512–525.

Andreae, M. O., and P. Merlet (2001), Emissions of trace gases and aerosols from biomass burning, *Global Biogeochem. Cycles*, *15*, 955–966.

Arino, O., M. Simon, I. Piccolini, and J. M. Rosaz (2001), The ERS-2 ATSR-2 World Fire Atlas and the ERS-2 ATSR-2 World Burnt Surface Atlas Projects, paper presented at 8th ISPRS Conference on Physical Measurement and Signatures in Remote Sensing, Int. Soc. of Photogramm. And Remote Sens., Aussois, France.

Auclair, A. N. D. (1985), Postfire regeneration of plant and soil organic pools in a *Picea mariana-Cladonia stellaris* ecosystem, *Can. J. For. Res.*, *15*, 279–291.

Bawkin, P. S., P. Tans, and P. C. Novelli (1994), Carbon monoxide budget in the Northern Hemisphere, *Geophys. Res. Lett.*, *21*, 433–436.

Benscoter, B. W., and R. K. Wieder (2003), Variability in organic matter lost by combustion in a boreal bog during the 2001 Chisholm fire, *Can. J. For. Res.*, *33*, 2509–2513.

Bradley, K. S., D. H. Stedman, and G. A. Bishop (1999), A global inventory of carbon monoxide emissions from motor vehicles, *Chemosphere Global Change Sci.*, *1*, 65–72.

Cahoon, D. R., Jr., B. J. Stocks, J. S. Levine, W. R. Cofer III, and J. A. Barber (1996), Monitoring the 1992 forest fires in the boreal ecosystem using NOAA AVHRR satellite imagery, in *Biomass Burning and Climate Change*, vol. 2, *Biomass Burning in South America, Southeast Asia, and Temperate and Boreal Ecosystems, and the Oil Fires of Kuwait*, edited by J. S. Levine, pp. 795–802, MIT Press, Cambridge, Mass.

Cofer, W. R., III, J. S. Levine, E. L. Winstead, and B. J. Stocks (1990), Gaseous emissions from Canadian boreal forest fires, *Atmos. Environ., Part A*, *24*(7), 1653–1659.

Cofer, W. R., III, E. L. Winstead, B. J. Stocks, D. R. J. Cahoon, J. G. Goldammer, and J. S. Levine (1996a), Composition of smoke from North American boreal forest fires, in *Fire in Ecosystems of Boreal Eurasia*, edited by J. G. Goldammer and V. V. Furyaev, pp. 465–475, Springer, New York.

Cofer, W. R., III, E. L. Winstead, B. J. Stocks, L. W. Overbay, J. G. Goldammer, D. R. Cahoon, and J. S. Levine (1996b), Emissions from boreal forest fires: Are the atmospheric impacts underestimated?, in *Biomass Burning and Climate Change*, vol. 2, *Biomass Burning in South America, Southeast Asia, and Temperate and Boreal Ecosystems, and the Oil Fires of Kuwait*, edited by J. S. Levine, pp. 834–839, MIT Press, Cambridge, Mass.

Cofer, W. R., III, E. L. Winstead, B. J. Stocks, J. G. Goldammer, and D. R. Cahoon (1998), Crown fire emissions of CO_2, CO, H_2, CH_4 and TNMHC from a dense jack pine boreal forest fire, *Geophys. Res. Lett.*, *25*, 3919–3922.

Conard, S. G., and G. A. Ivanova (1998), Wildfire in Russian boreal forests—Potential impacts of fire regime characteristics on emissions and global carbon balance estimates, *Environ. Pollut.*, *98*, 305–313.

Daniel, J. S., and S. Solomon (1998), On the climate forcing of carbon monoxide, *J. Geophys. Res.*, *103*, 13,249–13,260.

Dlugokencky, E. J., B. P. Walter, K. A. Masarie, P. M. Lang, and E. S. Kasischke (2001), Measurements of an anomalous global methane increase during 1998, *Geophys. Res. Lett.*, *28*, 499–502.

Duncan, B. N., R. V. Martin, A. C. Staudt, R. Yevich, and J. A. Logan (2003a), Interannual and seasonal variability of biomass burning emissions constrained by satellite observations, *J. Geophys. Res.*, *108*(D2), 4100, doi:10.1029/2002JD002378.

Duncan, B. N., I. Bey, M. Chin, L. J. Mickley, T. D. Fairlie, R. V. Martin, and H. Matsueda (2003b), Indonesian wildfires of 1997: Impact on tropospheric chemistry, *J. Geophys. Res.*, *108*(D15), 4458, doi:10.1029/2002JD003195.

Eva, H., and E. F. Lambin (1998), Remote sensing of biomass burning in tropical regions: Sampling issues and multisensor approach, *Remote Sens. Environ.*, *64*(3), 292–315.

FIRESCAN Science Team (1996), Fire in ecosystems of boreal Eurasia: The Bor Forest Island fire experiment fire research campaign Asia-north (FIRESCAN), in *Biomass Burning and Climate Change*, vol. 2, *Biomass Burning in South America, Southeast Asia, and Temperate and Boreal Ecosystems, and the Oil Fires of Kuwait*, edited by J. L. Levine, pp. 848–873, MIT Press, Cambridge, Mass.

Food and Agriculture Organization (1999), Forest fire statistics, *Timber Bull.*, *LII*(4), 19 pp.

Forster, C., et al. (2001), Transport of boreal forest fire emissions from Canada to Europe, *J. Geophys. Res.*, *106*, 22,887–22,906.

Frandsen, W. H. (1991), Burning rate of smoldering peat, *Northwest Sci.*, *65*, 166–172.

Fraser, R. H., Z. Li, and J. Cihlar (2000), Hotspot and NDVI differencing synergy (HANDS): A new technique for burned area mapping over boreal forest, *Remote Sens. Environ.*, *74*(3), 362–376.

French, N. H. F., E. S. Kasischke, B. J. Stocks, J. P. Mudd, D. L. Martell, and B. S. Lee (2000), Carbon release from fires in the North American boreal forest, in *Fire, Climate Change, and Carbon Cycling in the Boreal Forest*, edited by E. S. Kasischke and B. J. Stocks, pp. 377–388, Springer, New York.

French, N. H. F., E. S. Kasischke, and D. G. Williams (2002), Variability in the emission of carbon-based trace gases from wildfire in the Alaskan boreal forest, *J. Geophys. Res.*, *107*, 8151, doi:10.1029/2001JD000480. [printed *108*(D1), 2003]

French, N. H. F., P. Goovaerts, and E. S. Kasischke (2004), Uncertainty in estimating carbon emissions from boreal forest fires, *J. Geophys. Res.*, *109*, D14S08, doi:10.1029/2003JD003635.

Giglio, L., J. D. Kendall, and C. J. Tucker (2000), Remote sensing of fires with the TRMM VIRS, *Int. J. Remote Sens.*, *21*, 203–207.

Harden, J. W., K. P. O'Neill, S. E. Trumbore, H. Veldhuis, and B. J. Stocks (1997), Moss and soil contributions to the annual net carbon flux of a maturing boreal forest, *J. Geophys. Res.*, *102*, 28,805–28,816.

Harden, J. W., J. C. Neff, D. V. Sandberg, M. R. Turetsky, R. Ottmar, G. Gleixner, T. L. Fries, and K. L. Manies (2004), Chemistry of burning the forest floor during the FROSTFIRE experimental burn, interior Alaska, 1999, *Global Biogeochem. Cycles*, *18*, GB3014, doi:10.1029/2003GB002194.

Hoelzemann, J. J., M. G. Schultz, G. P. Brasseur, and C. Granier (2004), Global Wildland Fire Emission Model (GWEM): Evaluating the use of global area burnt data, *J. Geophys. Res.*, *109*, D14S04, doi:10.1029/2003JD003666.

Isaev, A. P., et al. (2002), Using remote sensing for assessment of forest wildfire carbon emissions, *Clim. Change*, *55*, 231–255.

Ito, A., and J. E. Penner (2004), Global estimates of biomass burning based on satellite imagery for the year 2000, *J. Geophys. Res.*, *109*, D14S05, doi:10.1029/2003JD004423.

Justice, C. O., et al. (2002), The MODIS fire products, *Remote Sens. Environ.*, *83*, 244–262.

Kajii, Y., et al. (2002), Boreal forest fires in Siberia in 1998: Estimation of area burned and emissions of pollutants by advanced very high resolution radiometer satellite data, *J. Geophys. Res.*, *107*(D24), 4745, doi:10.1029/2001JD001078.

Kasischke, E. S., and L. P. Bruhwiler (2002), Emissions of carbon dioxide, carbon monoxide, and methane from boreal forest fires in 1998, *J. Geophys. Res.*, *107*, 8146, doi:10.1029/2001JD000461. [printed *108*(D1), 2003]

Kasischke, E. S., N. L. Christensen, and E. Haney (1994), Modeling of geometric properties of loblolly pine tree and stand characteristics for use in radar backscatter models, *IEEE Trans. Geosci. Remote Sens.*, *32*, 800–822.

Kasischke, E. S., N. H. F. French, L. L. Bourgeau-Chavez, and N. L. Christensen Jr. (1995), Estimating release of carbon from 1990 and 1991 forest fires in Alaska, *J. Geophys. Res.*, *100*, 2941–2951.

Kasischke, E. S., K. P. O'Neill, N. H. F. French, and L. L. Bourgeau-Chavez (2000), Controls on patterns of biomass burning in Alaskan boreal forests, in *Fire, Climate Change, and Carbon Cycling in the North American Boreal Forest*, edited by E. S. Kasischke and B. J. Stocks, pp. 173–196, Springer, New York.

Kasischke, E. S., D. Williams, and D. Barry (2002), Analysis of the patterns of large fires in the boreal forest region of Alaska, *Int. J. Wildland Fire*, *11*, 131–144.

Kasischke, E. S., J. H. Hewson, B. Stocks, G. van der Werf, and J. Randerson (2003), The use of ATSR active fire counts for estimating relative patterns of biomass burning: A study from the boreal forest region, *Geophys. Res. Lett.*, *30*(18), 1969, doi:10.1029/2003GL017859.

Khalil, M., and R. A. Rasmussen (1994), Global decrease in atmospheric carbon monoxide, *Nature*, *370*, 639–641.

Kondo, Y., et al. (2003), Effects of biomass burning and lightning on atmospheric chemistry over Australia and South-east Asia, *Int. J. Wildland Fire*, *12*, 271–281.

Lacelle, B., C. Tarnocai, S. Waltman, J. Kimble, F. Orozco-Chavez, and B. Jakobsen (1997), North American soil carbon map, report, Agric. and Agri-food Can., Ottawa.

Langenfelds, R. L., R. J. Francey, B. C. Pak, L. P. Steele, J. Lloyd, C. M. Trudinger, and C. E. Allison (2002), Interannual growth rate variations of atmospheric CO_2 and its $\delta^{13}C$, H_2, CH_4, and CO between 1992 and 1999 linked to biomass burning, *Global Biogeochem. Cycles*, *16*(3), 1048, doi:10.1029/2001GB001466.

Lavoue, D., C. Liousse, H. Cachier, B. J. Stocks, and J. G. Goldammer (2000), Modeling of carbonaceous particles emitted by boreal and temperate wildfires at northern latitudes, *J. Geophys. Res.*, *105*, 26,871–26,890.

Leenhouts, B. (1998), Assessment of biomass burning in the conterminous United States, *Conserv. Ecol.*, *2*, 1–23.

Lowe, J. J., K. Power, and M. W. Marsan (1996), Canada's Forest Inventory 1991: Summary by terrestrial ecozones and ecoregions, Pac. For. Cent., Can. For. Serv., Victoria, B. C., Can.

Matsueda, H., and H. Y. Inoue (1999), Aircraft measurements of trace gases between Japan and Singapore in October of 1993, 1996, and 1997, *Geophys. Res. Lett.*, *26*, 2413–2416.

McRae, D. J. et al. (2005), Variability of fire behavior, fire effects, and emissions in Scotch pine forests of Central Siberia, *Mitigation and Adaptation Strategies for Global Change*, in press.

Michalek, J. L., N. H. F. French, E. S. Kasischke, R. D. Johnson, and J. E. Colwell (2000), Using Landsat TM data to estimate carbon release from burned biomass in an Alaskan spruce complex, *Int. J. Remote Sens.*, *21*, 323–338.

Miyanishi, K. (2001), Duff consumption, in *Forest Fire: Behavior and Ecological Effects*, edited by E. A. Johnson and K. Miyanishi, pp. 437–475, Elsevier, New York.

Novelli, P. C., K. A. Masarie, P. P. Tans, and P. M. Lang (1994), Recent changes in atmospheric carbon-monoxide, *Science*, *263*, 1587–1590.

Novelli, P. C., K. A. Masarie, P. M. Lang, B. D. Hall, R. C. Myers, and J. W. Elkins (2003), Reanalysis of tropospheric CO trends: Effects of the 1997–1998 wildfires, *J. Geophys. Res.*, *108*(D15), 4464, doi:10.1029/2002JD003031.

Schlesinger, P., and T. Stone (2001), Forest and landcover data of Russia and the former Soviet Union [CD-ROM], Woods Hole Res. Cent., Woods Hole, Mass. (Available at http://www.whrc.org)

Schultz, M. G. (2002), On the use of ATSR fire count data to estimate the seasonal and interannual variability in vegetation fire emissions, *Atmos. Chem. Phys.*, *2*, 387–395.

Seiler, W., and P. J. Crutzen (1980), Estimates of gross and net fluxes of carbon between the biosphere and atmosphere, *Clim. Change*, *2*, 207–247.

Shvidenko, A. Z., and S. Nilsson (2000), Fire and the carbon budget of Russian forests, in *Fire, Climate Change, and Carbon Cycling in the Boreal Forest*, edited by E. S. Kasischke and B. J. Stocks, pp. 289–311, Springer, New York.

Simon, M., S. Plummer, F. Fierens, J. J. Hoelzemann, and O. Arino (2004), Burnt area detection at global scale using ATSR-2: The GLOBSCAR products and their qualifications, *J. Geophys. Res.*, *109*, D14S02, doi:10.1029/2003JD003622.

Skinner, W. R., B. J. Stocks, D. L. Martell, B. Bonsal, and A. Shabbar (1999), The association between circulation anomalies in the mid-troposphere and area burned by wildland fire in Canada, *Theor. Appl. Climatol.*, *63*, 89–105.

Skinner, W. R., M. D. Flannigan, B. J. Stocks, B. M. Wotton, J. B. Todd, J. A. Mason, K. A. Logan, and E. M. Bosch (2002), A 500 hPa synoptic wildland fire climatology for large Canadian forest fires, 1959–1996, *Theor. Appl. Climatol.*, *63*, 89–105.

Soja, A. J., W. R. Cofer, H. H. Shugart, A. I. Sukhinin, P. W. Stackhouse Jr., D. J. McRae, and S. G. Conard (2004), Estimating fire emissions and disparities in boreal Siberia (1998–2002), *J. Geophys. Res.*, *109*, D14S06, doi:10.1029/2004JD004570.

Stocks, B. J. (1980), Black spruce crown fuel weights in northern Ontario, *Can. J. For. Res.*, *10*, 498–501.

Stocks, B. J. (1987), Fire behavior in immature jack pine, *Can J. For. Res.*, *17*, 80–86.

Stocks, B. J. (1989), Fire behavior in mature jack pine, *Can. J. For. Res.*, *19*, 783–790.

Stocks, B. J., and J. B. Kauffman (1997), Biomass consumption and behavior of wildland fires in boreal, temperate, and tropical ecosystems: Parameters necessary to interpret historic fire regimes and future fire scenarios, in *Sediment Records of Biomass Burning and Global Change*, edited by J. S. Clark, pp. 169–188, Springer, New York.

Stocks, B. J., et al. (2002), Large forest fires in Canada, 1959–1997, *J. Geophys. Res.*, *107*, 8149, doi:10.1029/2001JD000484. [printed *108*(D1), 2003].

Stolbovoi, V., and I. McCallum (2002), Land resources of Russia [CD-ROM], Int. Inst. for Appl. Syst. Anal., Laxenburg, Austria. (Available at http://www.iiasa.ac.at/Research/FOR/russia_cd/guide.htm)

Sukhinin, A. I., et al. (2004), Satellite-based mapping of fires in Eastern Russia: New products for fire management and carbon cycle studies, *Remote Sens. Environ.*, *93*, 546–564.

Tansey, K., et al. (2004), Vegetation burning in the year 2000: Global burned area estimates from SPOT VEGETATION data, *J. Geophys. Res.*, *109*, D14S03, doi:10.1029/2003JD003598.

Tarnocai, C. (1997), The amount of organic carbon in various soil orders and ecological provinces in Canada, in *Soil Processes and the Carbon Cycle*, edited by R. Lal et al., pp. 81–92, CRC Press, Boca Raton, Fla.

Thompson, A. M. (1992), The oxidizing capacity of the atmosphere: Probable past and future changes, *Science*, *256*, 1157–1165.

Turetsky, M. R., and R. K. Wieder (2001), A direct approach to quantifying organic matter lost as a result of peatland wildfire, *Can. J. For. Res.*, *31*, 363–366.

Turetsky, M. R., B. D. Amiro, E. Bosch, and J. S. Bhatti (2004), Peatland burning and its relationship to fire weather indices in western Canada, *Global Biogeochem. Cycles.*, *18*, GB4014, doi:10.1029/2004GB002222.

van der Werf, G. R., J. T. Randerson, G. J. Collatz, and L. Giglio (2003), Carbon emissions from fires in tropical and sub-tropical ecosystems, *Global Change Biol.*, *9*, 547–562.

van der Werf, G. R., J. T. Randerson, G. J. Collatz, L. Giglio, P. S. Kasibhatla, A. Arellano, S. C. Olsen, and E. S. Kasischke (2004), Continental-scale partitioning of fire emissions during the 97/98 El Niño, *Science*, *303*, 73–76.

Wirth, C., et al. (1999), Above-ground biomass and structure of pristine Siberian Scots pine forests as controlled by competition and fire, *Oecologia*, *121*, 66–80.

Wotawa, G., P. C. Novelli, G. Trainer, and C. Granier (2001), Inter-annual variability of summertime CO concentrations in the Northern Hemisphere explained by boreal forest fires in North America and Russia, *Geophys. Res. Lett.*, *28*, 4575–4579.

Yokelson, R. J., R. Susott, D. E. Ward, J. Reardon, and D. W. T. Griffith (1997), Emissions from smoldering combustion of biomass measured by open-path Fourier transform infrared spectroscopy, *J. Geophys. Res.*, *102*, 18,865–18,877.

Yurganov, L., et al. (2004), A quantitative assessment of the 1998 carbon monoxide emission anomaly in the Northern Hemisphere based on total column and surface concentration measurements, *J. Geophys. Res.*, *109*, D15305, doi:10.1029/2004JD004559.

Zander, R., P. Demoulin, D. H. Enhalt, U. Schmidt, and C. P. Rinsland (1989), Secular increase of total vertical column abundance of carbon monoxide above central Europe since 1950, *J. Geophys. Res.*, *94*, 11,021–11,028.

L. P. Bruhwiler and P. C. Novelli, Climate Modeling and Diagnostics Laboratory, NOAA, Boulder, CO 80305, USA. (lori.p.bruhwiler@noaa.gov; paul.c.novelli@noaa.gov)

N. H. F. French, Altarum, PO Box 134001, Ann Arbor, MI 48113-4001, USA. (nancy.french@altarum.org)

J. H. Hewson, E. J. Hyer, and E. S. Kasischke, Department of Geography, University of Maryland, College Park, 2181 LeFrak Hall, College Park, MD 20742, USA. (j.hewson@conservation.org; ehyer@glue.umd.edu; ekasisch@geog.umd.edu)

B. J. Stocks, Canadian Forest Service, 1219 Queen Street East, Sault Ste. Marie, Ont. P6A 2E5, Canada. (bstocks@nrcan.gc.can)

A. I. Sukhinin, Sukachev Forest Institute, Russian Academy of Sciences, Krasnoyarsk, Russia. (boss@ksc.krasn.rfus)